International Journal of Civil Engineering
https://doi.org/10.1007/s40999-023-00904-7

RESEARCH PAPER

Experimental Investigation of Soil Disturbance Effect on Bearing Capacity of Organic Soil

Cenk Cuma Çadır[1] · Zulkuf Kaya[2] · Hakan Yalcin[3] · Aykut Erol[2] · Erdal Uncuoğlu[2] · Muge Akin[3]

Received: 17 February 2023 / Revised: 26 August 2023 / Accepted: 21 September 2023
© The Author(s), under exclusive licence to the Iran University of Science and Technology 2023

Abstract
The model test investigations on the soft soils are usually carried out on samples prepared in the laboratory and assuming site conditions. However, such soils that are prepared in the laboratory only partially reflect the site conditions. Considering this gap in the literature, this study mainly focuses on the bearing capacity and settlement behavior of the undisturbed organic soil obtained by a novel block sampling technique. The disturbed organic soil prepared in the laboratory was investigated with large-scale model experiments for two different footing types (square and rectangular). Vane Shear testing (VST), Dynamic Cone Penetration (DCP) tests, and finite-element analysis (FEA) were performed. The average bearing capacity values of disturbed and undisturbed soil were 60.98 kPa–68.71 kPa and 108.18 kPa–110.89 kPa for square and strip footings, respectively. Bearing capacity reductions of up to 40% were determined on laboratory-prepared soils. The cone reached the required depth (450 mm) with three blows for disturbed soil, while it was reached with four blows for undisturbed soil. Likewise, the undrained shear strength obtained by the VST was determined as 22.16 kPa and 16.60 kPa for undisturbed and disturbed soils, respectively. Shear strength losses of up to 25% for disturbed soils were observed. The bearing capacity values obtained from FEA were comparable to those obtained with the model tests. It was concluded that the degree of degradation of organic soils in the laboratory significantly affects the bearing capacity of the soil.

Keywords Organic soil · Undisturbed soil sample · Model test · Field test · PLAXIS 3D

✉ Zulkuf Kaya
zkaya@erciyes.edu.tr

Cenk Cuma Çadır
cenk.cadir@bozok.edu.tr

Hakan Yalcin
hakan.yalcin@agu.edu.tr

Aykut Erol
aykuterol@erciyes.edu.tr

Erdal Uncuoğlu
erdalu@erciyes.edu.tr

Muge Akin
muge.akin@agu.edu.tr

[1] Department of Civil Engineering, Yozgat Bozok University, Yozgat, Turkey

[2] Department of Civil Engineering, Erciyes University, Kayseri, Turkey

[3] Department of Civil Engineering, Abdullah Gul University, Kayseri, Turkey

1 Introduction

Soft soils, such as organic soils, can cause permanent damage to the carrier systems of the structures (Buildings, Bridges, Road Silos, etc.) on which they are built due to excessive, altering settlements and low bearing capacity. Organic soils are common in Turkey (Izmir, Kayseri, Yüksekova, Trabzon Ağaçbaşı Plateau, Abant Lake, Yesilırmak Delta, and Bolu) as well as all over the world (Canada, Russia, Malaysia, Indonesia, and America). Organic soils generally have high moisture content, organic matter content, permeability, void ratio, and high compressibility [1–3]. Since organic soil areas are generally located in regions that are flat, it has become common to establish extensive industrial facilities in these areas. The presence of organic soil the industrial facility area needs a detailed analysis of the soil type from a geotechnical point of view and the correct determination of the bearing

Published online: 11 October 2023

capacity problems that may occur. Researchers have carried out many studies on identifying and improving the geotechnical properties of organic soil [4–9]. Organic soil's index and geotechnical properties have been determined using disturbed and undisturbed soil samples. However, sample collection from the field as well as transportation and preparation mechanisms cause significant disturbance in the soil sample [10–12].

According to Karlsrud and Hernandez-Martinez [13] and Amundsen et al. [14, 15], soft soils are prone to sample disturbance, especially when samples are taken using tube samplers. Block sampling is a relatively safe procedure for such soils. The researchers stated that the deterioration during sampling with a tube is much greater than that of a block [11, 16]. It is reported that as the block sample size increases, the disturbance remains at the lowest level. In undrained test conditions, the possibility of disturbing organic soil samples may adversely affect the soil's shear strength. Therefore, collecting block samples for soft soils, such as soft clay and organic soil, is considered as the most effective approach to addressing this situation.

The block sampling method generally involves taking samples as blocks in an opened research pit by applying a specific procedure, as given below:

i) Careful hand digging of the ground around the sample and trimming a regular shaped block,
ii) Sealing the floor block with beeswax, and
iii) Enclosing and cutting the samples base followed by board placement [17].

Literature comprises various studies in which block sampling is used; however, horizontal stress must be zero while digging the surrounding soil—delicate handling must be ensured for the samples to be considered undisturbed. In this study, a novel variation is developed that combines the Shelby tube and block sampling approaches. Details are reported in the related sections. While samples are collected with a large-scale steel box, the wall thickness of the steel box is thin enough to disturb the sample minimally but thick enough to withstand the bending moment. In addition, the horizontal stress in the site is preserved, since the box penetrates the soil. A little disturbance near the box's inner side was observed but negligible, since the stress bulbs are dampened. Another advantage of this method is that the loading tests can be conducted without further processing complexities.

This study comprises three stages: sample collection, model testing, and comparative analysis testing of the disturbed organic soil (DOS) and undisturbed organic soil (UOS). Additionally, results were scrutinized with the numerical analysis.

The undisturbed samples (organic soils) were taken from the Kayseri Free Zone (KFZ) field, where generally single isolated or strip foundations are used for structures. It was noted that there resides a layer of sand immediately beneath the organic soil during the drilling exploration of the site. Taking the situation into account, the model tests were conducted by placing a sand layer under the organic soil using two boxes (750 mm × 750 mm × 300 mm and 1000 mm × 750 mm × 300 mm).

Model tests on the undisturbed organic soil (UOS) were carried out by loading footing of two sizes (240 mm × 240 mm × 20 mm and 420 mm × 80 mm × 20 mm). After the sample collection, bearing capacity and settlement values were obtained by loading the organic soil placed in steel boxes considering the site conditions. In addition to the model tests, Dynamic Cone Penetration (DCP) and Field Vane Shear (FVT) tests were also conducted to compare disturbed and undisturbed soils. At the last stage, the numerical analysis results obtained by modeling the loading tests performed under controlled laboratory conditions using the PLAXIS 3D program were compared with the model test results.

2 Materials

2.1 Organic Soils

The material under research is collected from the KFZ and the properties of the organic soil and its components were determined using various tests. The borehole log of the research site is given in Fig. 1. The soil profile consists of topsoil, organic soil (OS), silty sand, and low-plasticity clay. The model experiments were conducted on a profile consisting of two layers (OS (Layer I) and sand (Layer II)) to simulate the site conditions.

The grain size distribution curves of the OS and silty sand are given in Fig. 2. Samples were collected from the KFZ area at 1.2–1.7 m depth. The results obtained from the property determination tests (pycnometer test, Atterberg limit tests, laboratory compaction test, etc.) performed on the DOS and UOS samples are given in Table 1. While the organic soil of Kayseri is characterized as highly plastic organic clay (loss on ignition, LOI = 10%), it was determined that it contains 38% clay and 59% silt. The sand was classified as silty sand (SM-SC). As for the refined grain content, organic soil and sand contained at least 97% and 40% fine grains. Based on the unified soil classification system (USCS), organic soil is classified as high plasticity organic clay (OH).

X-ray fluorescence (XRF) analysis was performed on the OS samples to determine the components, as shown in Table 2.

Based on the XRF results and the properties of the soil given in Tables 1 and 2, it can be concluded that high silt



Fig. 1 Borehole log and test pit

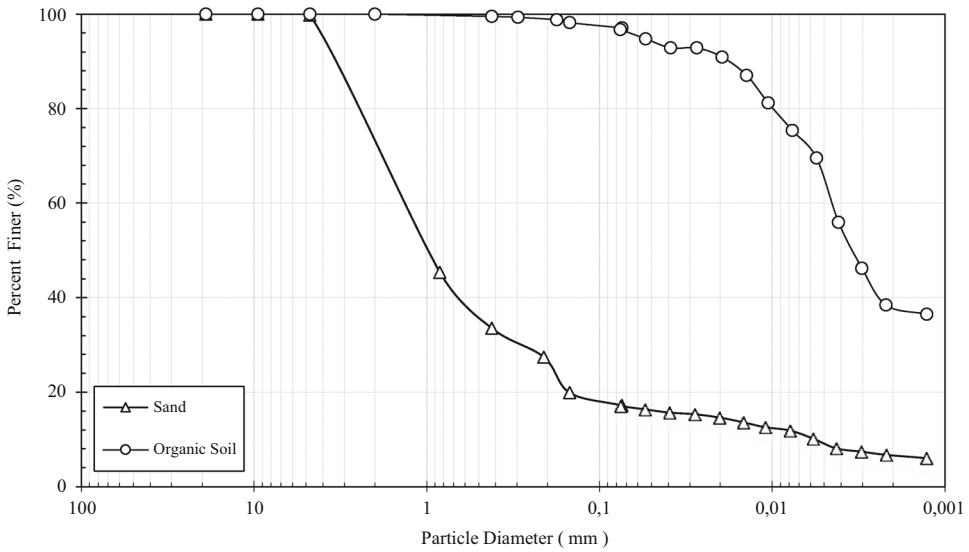

Fig. 2 Grain size distribution curves of testing soils

(Table 2: %61 silt) and fiber content (Table 1: %62 silt) may affect the internal friction angle value that is a crucial parameter for shear strength determination of OS [21, 22].

2.2 Sand

The grain size distribution of the sand (Layer II) under the OS (Layer I) used in the model tests is given in Fig. 2. The results of the pycnometer, direct shear, and permeability test performed on the sand are shown in Table 3. According to the unified soil classification system (USCS), the class of sand soil is determined as silty-clayey sand (SM-SC).

3 Test Program and Test Setup

Model tests were carried out on both layers, Layer I and Layer II represented the OS and sand (in both disturbed and undisturbed states), respectively. The undisturbed organic soil (UOS) was subjected to model loading tests for square and rectangular footings. Details of the dimensions used for the footings and for the test boxes are given in Table 4.

The frame system on which the loading tests were carried out is given in Fig. 3. The primary components of the system are the hydraulic loading jack (10-ton capacity) and load–displacement controlling unit (0.5–10 mm/min sensitivity). There is a 16-channel data logger that can simultaneously connect measuring elements, such as load cell (50 kN) soil pressure (2 MPa) and LVDT (100 mm).

Table 1 Physical properties of organic soil

Properties	Value
Moisture content (ω), % [18]	170.8
Specific gravity [19]	1.91
Liquid limit (LL), % [20]	211.2
Plastic limit (PL), % [20]	109.1
Index of plasticity (PI), %	102.1
Optimum moisture content (ω_{opt}), %	72
Maximum dry density ($\gamma_{d,max}$), kN/m^3	5.8
Unconfined compressive strength (q_u), kN/m^2	22.3
Cohesion (c_u), kN/m^2	11.2
Internal friction angle (ϕ), degree	34.9
Permeability coefficient (cm/sec)	1.52×10^{-7}
Unified soil classification system (USCS)	High plasticity organic clay (OH)
Von post classification system	H4-H6
Fiber content (FC), %	Hemic
Ash content (AC), %	High ash content (ash content % 38)

Table 2 The results of the XRF method's chemical analysis for organic soil

Name	(%)
SiO_2	61.219
CaO	16.181
Al_2O_3	9.864
Fe_2O_3	4.668
MgO	3.954
Na_2O	1.164
K_2O	1.111
TiO_2	0.583
P_2O_5	0.267
SO_3	0.160
SrO	0.100

In addition, on the left side of the frame system, there is a horizontal crane system with a capacity of 3 tons, which is used for removing the bottom cover of the test box.

Since the site explorations revealed presence of sand under the OS, tests were performed using two boxes (see Table 4) containing Layer I and Layer II, as shown in Fig. 3. The sand soil was beneath the OS. The sand soil layer's relative density, internal friction angle (ϕ), and cohesion value (c) are 60%, 41.20°, and 10.7 kPa, respectively. The dimensions of the sand boxes are given in

Table 3 Physical properties of sand soil

Soil type	Sand
Moisture content (w, %)	0.10
Specific gravity (γ_s, kN/m^3)	2.70
Cohesion (c, kN/m^2)	10.70
Internal friction angle (ϕ,°)	41.20
Permeability coefficient (k, cm/sn)	1.38×10^{-3}
Unified soil classification system (USCS)	Silty-clayey sand (SM-SC)

Fig. 4a in which the sand soil was inserted with successive blows as shown in Fig. 4b.

As for the boxes used for the block sampling, details are given in Fig. 5. These boxes were made of 10 mm-thick steel and consisted of three parts: the main body, the upper cover, and the lower cover (sled). Design was prepared with the intention to remove OS from the site without disturbing it. Other than the physical characteristics, design was enriched with the following features. Considering the pressure applied to the top cover to push the main body to the soil, the top cover is reinforced with steel elements. Air holes were opened on the top cover to allow the OS to be easily placed in the main body during the immersion of the test box into the soil. The lower parts of the main body are made at an angle of 30° for easier penetration into the OS. In addition, after placing the boxes on the soil, a movable bottom cover (sled) is used to contain the OS within the box.

Figure 6 shows the UOS collection process. Delicate handling was ensured for collecting the samples in an undisturbed way. As a first step, the topsoil surface was cleared, and a gradual excavation was carried out at 80 cm above the groundwater level. At the second stage, the test box's bottom cover (sled) was removed and boxes were placed on the OS at 50 cm horizontal intervals. At the third stage, the test boxes were penetrated into the OS resulting in the insertion of OS into the boxes. The test boxes' lower covers (sled) were replaced at the fourth stage. Finally, the test boxes were removed, wrapped with a nylon cover, and brought to the laboratory with extreme care and delicate handling.

One of the most critical aspects of this study is the determination of the disturbance status (quality) of the OS samples, so that they can be accepted as undisturbed. Therefore, to assess the disturbance of OS samples in block size, the methods proposed by Andresen and Kolstad [23], Lunne et al. [24], and Karlsrud and Hernandez-Martinez [13] were used. The criteria for the specified procedures are given in Table 5 in detail. Andresen and Kolstad stated that the soil disturbance might be related to the volume change

Table 4 Dimensions of footings and test boxes

Tested specimen	Test box dimensions	Sand box dimension	Footing type
Sand layer[1] + UOS[2]	750 mm × 750 mm × 450 mm	750 mm × 750 mm × 300 mm	Square[a]
	750 mm × 1000 mm × 450 mm	750 mm × 1000 mm × 300 mm	Rectangular[b]
Sand layer[1] + DOS[2]	750 mm × 750 mm × 450 mm	750 mm × 750 mm × 300 mm	Square[a]
	750 mm × 1000 mm × 450 mm	750 mm × 1000 mm × 300 mm	Rectangular[b]

[a]240 mm × 240 mm × 20 mm for square footing

[b]80 mm × 420 mm × 20 mm for rectangular footing

[1]Layer I (undisturbed-disturbed organic soil)

[2]Layer II (sand soil)

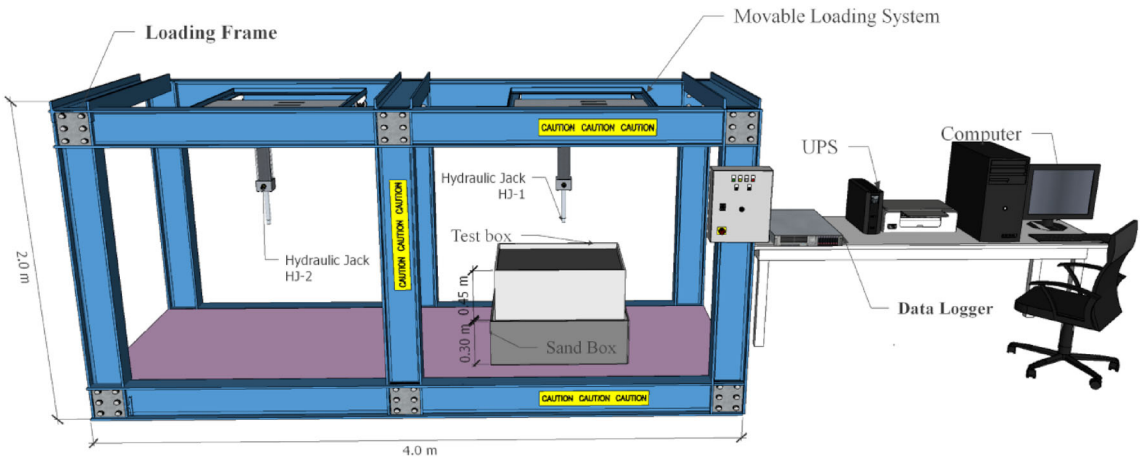

Fig. 3 3D view of the loading frame

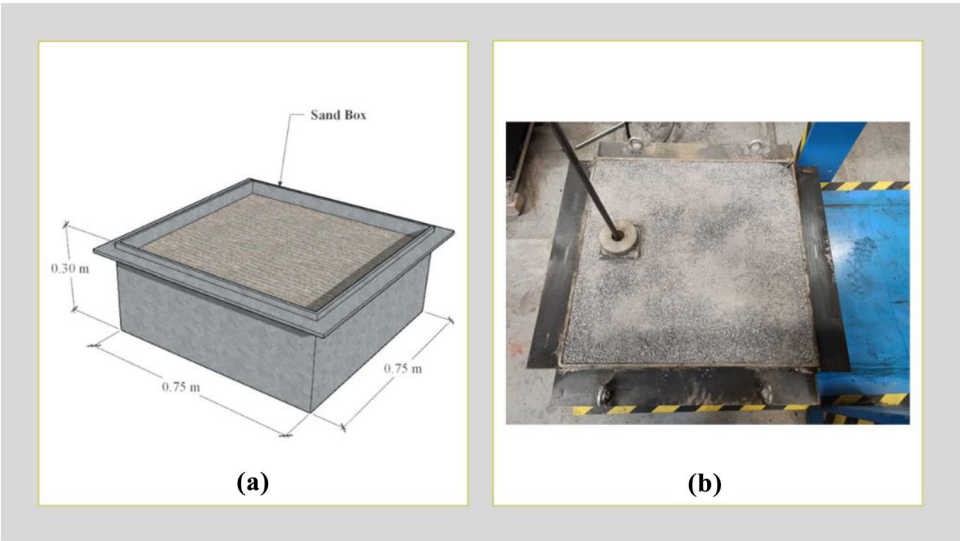

Fig. 4 The dimensions of the sandbox (**a**) and the compaction of the sand layer (**b**)

(ε_v) that occurred during the consolidation test. Lunne et al. [24] revealed that the disturbance of the soil sample might be related to the excessive consolidation rate (OCR) and the initial void ratio (e_0) [the change in void ratio due to the

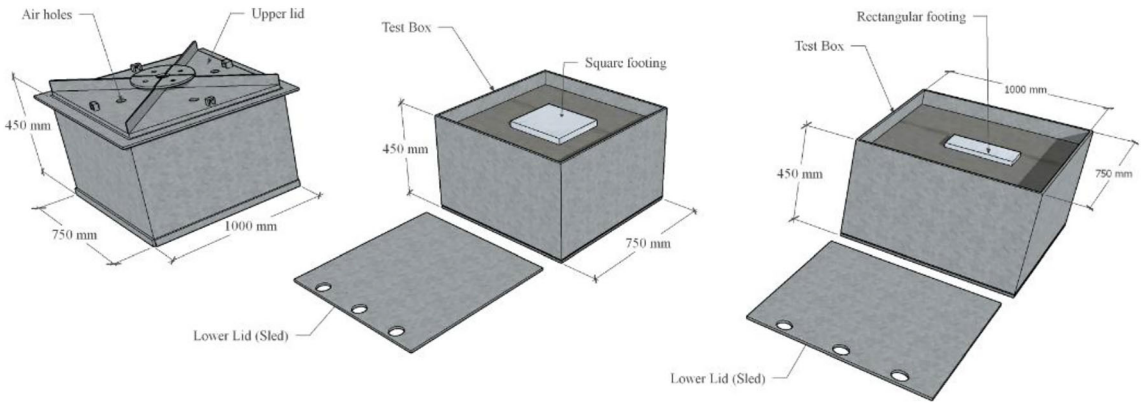

Fig. 5 Dimensions of model test boxes used for loading tests



Fig. 6 Undisturbed sampling process for organic soil

Table 5 The recommended methods for evaluating the disturbance of samples (quality) [25]

Method	Parameter	Sample quality			
		Very good to excellent	Good to fair	Poor	Very poor
Andresen and Kolstad [23]	ε_v	< 1	1–4	4–10	> 10
Lunne et al. [24] for OCR = 1–2	$\Delta e/e_0$	< 0.04	0.04–0.07	0.07–0.14	> 0.14
Lunne et al. [24] for OCR = 2–4	$\Delta e/e_0$	< 0.03	0.03–0.05	0.05–0.10	> 0.10
Karlsrud and Hernandez-Martinez [13]	M_0/M_L	> 2	1.5–2.0	1.0–1.5	< 1

ε_v = Volume change, e_0 = initial void ratio, OCR = over-consolidation ratio, Δe = change in void ratio, σ'_{v0} = effective stress, M_0/M_L = oedometer stiffness ratio

effective stress (σ'_{v0}) applied to the soil sample is (Δe)]. Karlsrud and Hernandez-Martinez [13] stated that the disturbance (quality) of the soil sample could be found based on the oedometer stiffness ratio obtained from the consolidation test results.

One-dimensional consolidation tests were carried out on the OS sample taken from the site as a block based on the criteria specified in Table 5 and in accordance with the ASTM D2435 standards [26]. Stresses ranging from 10 to 900 kPa were applied to 20 mm soil samples. As a result of the applied stresses, the average volumetric change rate (ε_v) was between 0.035 and 0.790; the normalized void rate change ($\Delta e/e_0$) and over-consolidation rate (OCR) were between 0.0097–0.0298 and 1.73–1.96, respectively; oedometer stiffness ratio (M_0/M_L) was obtained in the range of 1.987–2.623. Evaluating the results, it was

determined that the quality of the block OS samples taken with the help of test boxes was excellent and close to perfect (minimum disturbance).

The preparation of the disturbed organic soil (DOS) also followed a specific procedure (Fig. 7) of the following steps. DOS was placed in steel boxes based on the in-situ index properties (γ_n = 11.99 kN/m^3, e = 3.30, and ω = 171%) of the soil. The moisture content of the soils was determined (at least 5 samples) which was followed by inserting DOS in the plastic sacks. To match the moisture content of the samples with the site conditions, the missing water was added into the sample by correlating the volume and the weight of the DOS. Since the height of the box was 450 mm, the filling process was divided into three stages. Each stage covered the 150 mm height of the box by pouring the weight required to levitate the soil level by 150 mm. The soil surface was meticulously leveled to serve as a reference for any surface bulging and a line in the inner surface of the box was drawn. Each time after filling the soil till a 150 mm increment, a rammer (2.5 kg, 100 × 100 mm^2) was used for stroking the soil till the drawn line. Knowing that the bottom layers may get denser during the compacting of the top levels, lower layers of the soil in the test box were compacted with less force than the upper layers. The optimum number of strokes has been determined as 112 for each 150 mm increment. In addition to the 150 mm control line, natural unit volume weight values were determined for each level and compared with those in the site.

In all disturbed model experiments, organic soils were placed in test boxes with equal natural unit weight, relative density, and moisture content, which was followed by the conduction of the model test experiments. To control the site properties, the unit weight of soils was determined by taking tube samples of 100 mm height and 50 mm diameter from 3 points for each level (150 mm) and comparing them with the soil's natural unit weight values in the site. The relative density distribution was almost homogeneous, with a difference of less than 5–10% in the final compaction stage (top 150 mm increment). Although there was a minor increasing trend in relative density with depth, the upper part of the soil was quite close to the target relative density. This is significant, because the soil in this area will have the greatest influence on the surface footing reaction.

4 Model Tests and Results

The model tests were conducted on the UOS and DOS in two groups, with square and rectangular footings, with the presence of sand layer. The preparation process of the tested samples is already reported above, and details of the configuration are given in Table 4. Layer I (OS) and Layer II (sand) are both combined by sliding (removing) the sled under the test box which followed by surface smoothing with a fret saw. Two configurations (rectangular and square) of the footings were placed on the soil under which a soil pressure sensor was placed. Additionally, linear variable differential transformer (LVDTs) with 100 mm capacity were installed on both sides of the footing to take the settlement values. Moreover, soil pressure sensors were placed between the steel box walls and the organic soil, and it was made ready for the tests. Figure 8 shows the tests configurations for UOS (Fig. 8a, b) and DOS (Fig. 8c, d) with square and rectangular footings equipped with the above-mentioned sensors under loading.

Model tests were carried out with a 1 mm/min loading rate. In all model tests, the loadings were continued until a displacement of approximately 100 mm occurred (Fig. 9). All model tests were carried out within 36 h after they were taken from the site or prepared in the laboratory.

There have been reported various techniques for calculating the bearing capacity such as the 0.1B, log–log, tangent-intersect, and hyperbolic methods. For example, utilization of the stress (q) and settlement (s) values from the laboratory model tests has been reported [25, 27, 28]. Among these methods, the 0.1B method is considered



Fig. 7 Compaction of disturbed organic soil

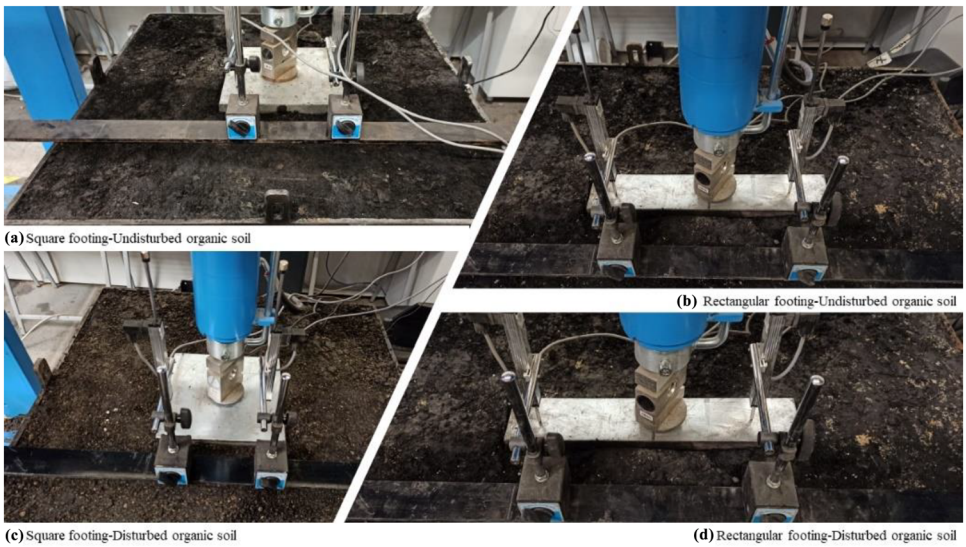

Fig. 8 Model loading test arrangement for undisturbed and disturbed conditions on the different footing styles; square footing (**a**–**c**) and rectangular footing (**b**–**d**)



Fig. 9 The top view of square (**a**) and rectangular (**b**) footing after the loading test

much reliable specially for inspecting failure curves produced during failure loads [29]. Thus, the 0.1B method was used to determine the final bearing capacity in this study. In the 0.1B method, the load value corresponding to 10% of the footing width (B) is accepted as the final bearing capacity value [30]. Stress-settlement graphs obtained as a result of all loading tests are given in Fig. 10. The average bearing capacity values of the DOS were determined as 60.98 kPa and 68.71 kPa for square and rectangular foundations, respectively. The average bearing capacity values of the UOS using the new block sampling technique were found to be 108.18 kPa and 110.89 kPa for square and rectangular foundations, respectively. The stress values corresponding to 10% of the width of the footing (24 mm for square footing and 8 mm for rectangular footing) according to the 0.1B method are given in Table 6.

It can be seen in Fig. 10 and Table 6 that the bearing capacity values of DOS are low compared to the UOS. To see the failure mechanisms of the organic soil under the footings, cross-sections were obtained after the loading tests, as shown in Fig. 11. The UOS developed shear failures predominantly at the footing edges and at the active and passive regions, similar to the local shear failure. As for the DOS, the footing settlement was similar to the punching fracture of the soil with the presence of indistinct cracks on the footing sides.

The pressure values obtained with the soil pressure transducers placed at various locations in the test box are given in Table 7.

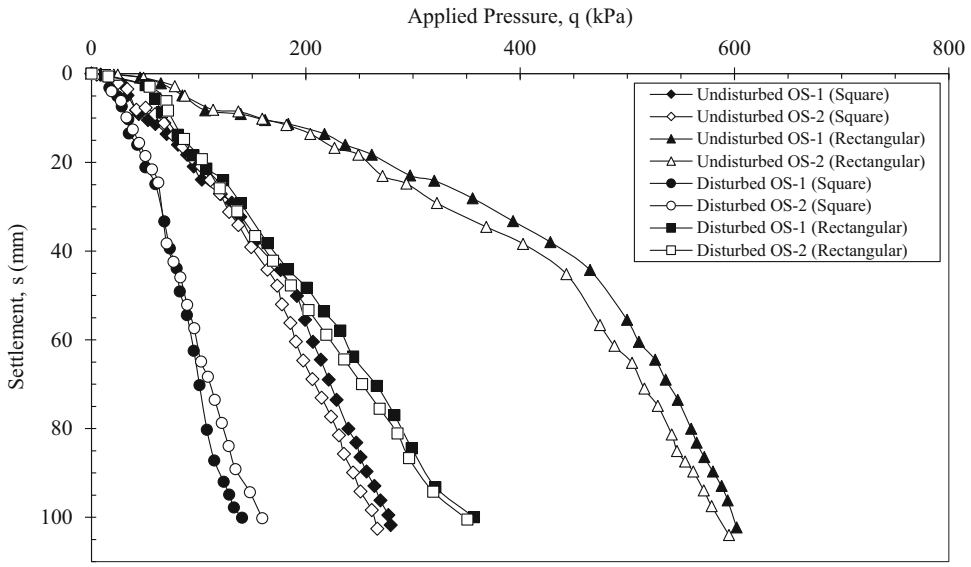

Fig. 10 Applied pressure-settlement curves of disturbed and undisturbed organic soils

Table 6 Bearing capacity values of disturbed and undisturbed organic soil

Loading tests	Bearing capacity (kPa		
	8 mm (0.1B)	24 mm (0.1B)	100 mm (Ultimate)
UOS-1S	–	105.24	278.15
UOS-2S	–	111.12	264.27
DOS-1S	–	59.65	126.43
DOS-2S	–	62.32	145.25
UOS-1R	108.19	–	599.12
UOS-2R	113.60	–	593.67
DOS-1R	66.12	–	321.04
DOS-2R	71.30	–	315.16

UOS-1S Undisturbed organic soil 1-square footing, *U* undisturbed, *D* disturbed, *1* test no, *S* square footing, *R* rectangular footing

Based on the results given in Table 7, the pressure under the footing changes in the range of 10.27 kPa and 19.37 kPa for the UOS. The pressure value under the footing in DOS varies between 11.08 kPa and 19.75 kPa. The pressure values measured between the OS layer and the sand layer changed between 4.77 kPa and 9.63 kPa in UOS, respectively, and 5.71 kPa to 9.87 kPa in DOS. While the pressure values measured at the steel frame boundaries changed between 1.12 kPa and 3.57 kPa for UOS and 1.67 kPa and 3.75 kPa for DOS.

4.1 Calculation of Bearing Capacity with Different Analytical Methods

Various methods can be used theoretically to determine the bearing capacity of the shallow foundations. According to the limit equilibrium approach proposed by Terzaghi [31], the ultimate bearing capacity of the soil is calculated according to Eq. (1) using different soil parameters (cohesion, friction angle, and unit weight of the soil)

$$q_u = k_1 \cdot c \cdot N_c + \gamma_1 \cdot D_f \cdot N_q + k_2 \cdot \gamma_2 \cdot B \cdot N_\gamma \quad (1)$$

Meyerhof [32] proposed an approach to find the forces that occur when punching a rigid-perfectly plastic material (Eq. 2)

$$q_u = c \cdot N_c \cdot s_c \cdot d_c \cdot i_c + q \cdot N_q \cdot s_q \cdot d_q \cdot i_q + 0.5 \cdot \gamma \cdot B \cdot N_\gamma \cdot s_\gamma \cdot d_\gamma \cdot i_\gamma. \quad (2)$$

Hansen [33] added factors such as embedment depth, load slope, eccentricity, surface slope, and footing shape in addition to Eq. 3

$$q_u = c \cdot N_c \cdot s_c \cdot d_c \cdot i_c \cdot b_c \cdot g_c + q \cdot N_q \cdot s_q \cdot d_q \cdot i_q \cdot b_q \cdot g_q + 0.5 \cdot \gamma \cdot B \cdot N_\gamma \cdot s_\gamma \cdot d_\gamma \cdot i_\gamma \cdot b_\gamma \cdot g_\gamma \quad (3)$$

Skempton [34] proposed an approach based on the undrained shear strength of the soil (Eq. 4)

$$q_u = c_u \cdot N_c = 9 \cdot c_u \quad (4)$$

It is recommended to use decreased shear strength parameters under weak soil properties such as local shear in the soil, punching shear failure, or $c_u < 100$ kPa (Eq. 5)

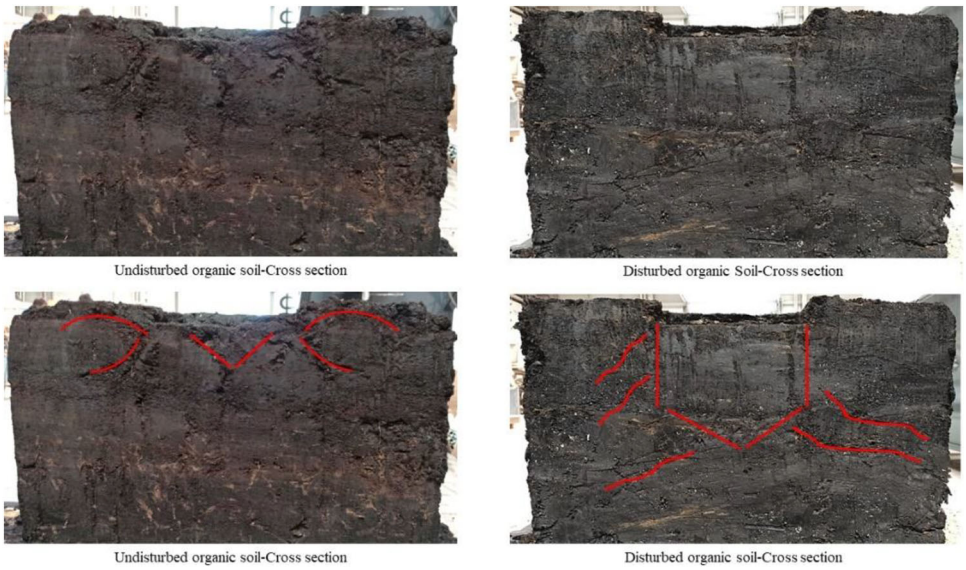

Fig. 11 Views from the cross-sections of the disturbed and undisturbed organic soils

Table 7 Pressure values obtained from the soil pressure transducer

Test info	Settlement (mm)	Pressure below footing (kPa)	Pressure between the layer of organic soil and sand (kPa)	Pressure at the boundaries of the test box (kPa)	
				Length of the box (kPa)	Width of the box (kPa)
UOS-1S	24 mm	10.27	4.77	2.23	–
	100 mm	20.12	9.63	3.21	–
UOS-2S	24 mm	11.35	5.49	1.97	–
	100 mm	21.45	11.09	3.09	–
UOS-1R	8 mm	11.92	5.78	1.12	2.08
	100 mm	17.73	9.98	2.65	3.19
UOS-2R	8 mm	13.49	6.29	1.42	2.29
	100 mm	18.69	10.04	2.63	3.61
DOS-1S	24 mm	11.39	5.97	2.96	–
	100 mm	19.49	9.87	3.69	–
DOS-2S	24 mm	11.08	5.71	3.02	–
	100 mm	19.75	9.59	3.47	–
DOS-1S	8 mm	12.24	6.11	1.67	2.21
	100 mm	17.93	9.08	2.83	3.64
DOS-2R	8 mm	12.64	6.45	1.96	2.43
	100 mm	18.08	9.77	3.09	3.75

UOS-1S: Undisturbed organic soil 1-square footing, *U* undisturbed, *D* disturbed, *1* test no, *S* square footing, *R* rectangular footing

$$c' = 0.67 \times c \rightarrow \tan\phi' = 0.67 \times \tan\phi, \quad (5)$$

where c is the cohesion, c_u is the undrained shear strength, k_1 and k_2 are the foundation shape factors, D_f is the depth of the foundation base, γ_1 is the unit weight of soil above the foundation base, γ_2 is the unit weight of the soil below foundation base, B is the footing width, N_c, N_q, and N_γ are bearing capacity factors, s_c, s_q, and s_γ are the shape factors, i_c, i_q and, i_γ are load inclination factors, d_c, d_q, and d_γ are depth factors, b_c, b_q, and b_γ are the base inclination factors, and g_c, g_q, and g_γ are the ground inclination factors.

The bearing capacity values of OS in this investigation were determined empirically using Eq. 5 (Table 8).

4.2 Field Tests and Results

Dynamic Cone Penetration test (DCP) and Field Vane test (FVT) tests were carried out to determine the effect of disturbance on the strength parameters of the soil in the study area. DCP and FVT tests were conducted on OS in three conditions: OS in the site, UOS taken from the site with the help of a test box, and OS prepared by disturbing in a test box in the laboratory.

The DCP test is an easy-to-apply and fast-resulting test that measures the penetration resistance of the soil [35, 36].

Table 8 Bearing capacity values of organic soil according to different methods

Empirical methods	Bearing capacity values (kPa)	
	Square footing	Rectangular footing
Terzaghi equation	82.99	63.84
Meyerhof equation	63.84	63.84
Hansen equation	75.97	65.97
Skempton equation	63.84	63.84

The first application of the DCP test as a portable device was used in 1956 [37]. The penetration values were taken from the site, and UOS and DOS are given in Fig. 12 according to ASTM D6951-18 [38]. According to the test results, number of blows (N) vs. depth (mm) values were given in Fig. 13.

The number of blows (N) vs. depth (mm) values are given in Fig. 13. DCP tests were performed at both site and laboratory. A depth of 400 mm was reached in 4 blows for UOS, and a depth of 400 mm was achieved in 3 blows for DOS, respectively. When the test results in Fig. 13 are examined, it can be seen that a depth of 400 mm (steel frame height) was attained in four strokes during the DCP tests conducted on the field and on the box from which undisturbed organic soils were collected. The number of hits in the DCP method decreases when the soil strength increases. This study shows that the internal structure of DOS deteriorates, as seen by the decline in the number of impacts on undisturbed organic soils. The bearing capacity value is lowered due to the soil's decreased resistance to the tapered tip. The FVT is a method developed to determine the undrained shear strength of the saturated clays with an undrained shear strength of 0–200 kN/m^2. It is also used in test silts, organic soils, and waste sludge. In this study, readings were taken from six different points, from the depth at which undisturbed organic soil was taken from the site, based don ASTM D2573 standard, and from test boxes containing UOS and DOS (Fig. 14). The undrained shear strength values obtained from these tests are given in Table 9.

Table 9 shows a 1.5% difference between the vane test results taken from the OS at site and the test box taken from the site as a block. However, it was determined that there were differences of up to 26% between the DOS vane test results prepared in the laboratory and the vane test results applied in other conditions.

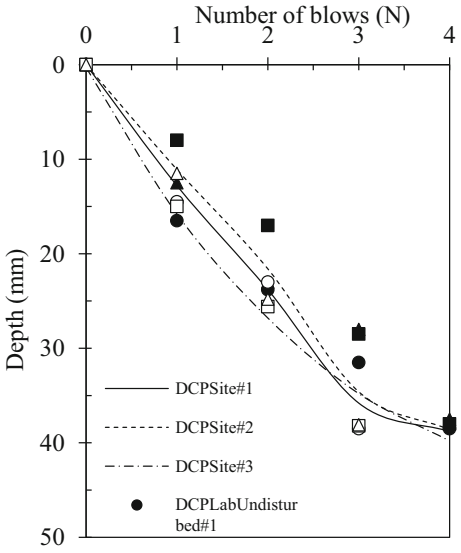

Fig. 13 Cone penetration depth depends on the number of blows

5 Numerical Analysis and Results

The finite-element technique has recently been widely used to solve geotechnical engineering problems [39]. In this part of the study, organic soils' settlement and bearing capacity under shallow foundations were analyzed using PLAXIS 3D software, a non-linear finite-element program. The soft soil model was used as a material model in the FE analysis. The material manual of PLAXIS 3D suggests that near-normally consolidated clays, clayey silts, and peat offer a soft soil model that represents the settlement

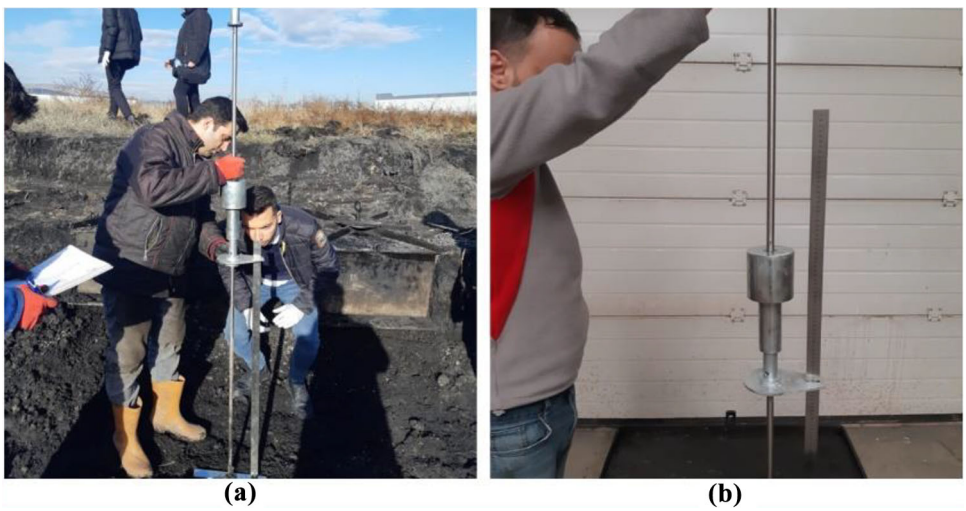

Fig. 12 Implementation of the DCP test at site (**a**) and laboratory (**b**)



Fig. 14 Implementation of the Vane shear test in the site and laboratory

Table 9 Vane shear test results of organic soil

Test no	Undrained cohesion (kPa)		
	Site test	Lab test-UOS	Lab test-DOS
1	17.7	25.6	17.5
2	30.5	20.3	16.0
3	29.6	24.0	17.2
4	25.5	19.2	15.5
5	21.8	27.2	17.3
6	20.5	25.1	15.7
7	17.9	21.9	16.5
8	21.2	18.7	16.9
9	18.1	17.6	17.1
Mean	22.5	22.2	16.6

behavior much better due to the high compressibility of OS. In addition, soft soil model is widely used in the literature [40–44]. It was determined that the most suitable drainage type for the soft soil model would be undrained (A) [45]. In this study, oedometer tests were performed, and values for the modified compression index (λ^*) and modified swelling index (κ^*) were determined. Also, direct shear tests were performed to get the strength parameters of OS. In the soft soil model, PLAXIS 3D has only the Undrained (A) option for drainage type. The material properties of the OS and sand used in the numerical analysis and other related parameters are given in Table 10.

Soils are modeled as triangular elements with ten nodes in the FE analysis. The choice of mesh size is essential in the compatibility of FE analysis with model tests. For this reason, a convergence study was conducted for the most

Table 10 Material properties of testing soils for FE analysis

Material properties	Organic soil	Sand
Material model	Soft soil	Mohr–Coulomb
Material behavior	Undrained (A)	Drained
Unit weight above phreatic level, γ_{unsat} (kN/m^3)	11.99	16.90
Unit weight below phreatic level, γ_{sat} (kN/m^3)	12.12	20.30
Young's modulus, E (kN/m^2)	–	30×10^3
Poisson ratio, ν	–	0.30
Cohesion, c (kN/m^2)	9.50	10.70
Friction angle, ϕ (°)	34.90	41.20
Dilatancy angle, Ψ (°)	–	11.20
λ (Lambda)	0.20	–
κ (Kappa)	0.04	–

appropriate mesh size in the analyses. Due to the sensitive stress-settlement conditions under the footing, the mesh density increases in at that region, as shown in Fig. 15.

The vertical displacement change after numerical analysis is given in Fig. 16.

The PLAXIS 3D program was used to evaluate the data, and it was determined that the highest displacement happened immediately below the foundation plate. However, a 20–30 mm swelling occurred on all four sides of the square foundation plate and only along the long side of the rectangular footing. In addition, it is seen that near-zero displacement occurs at the steel box boundaries and sand soil layer, while permanent displacements toward the bottom of the box decrease (Fig. 16). It can be said that the soil

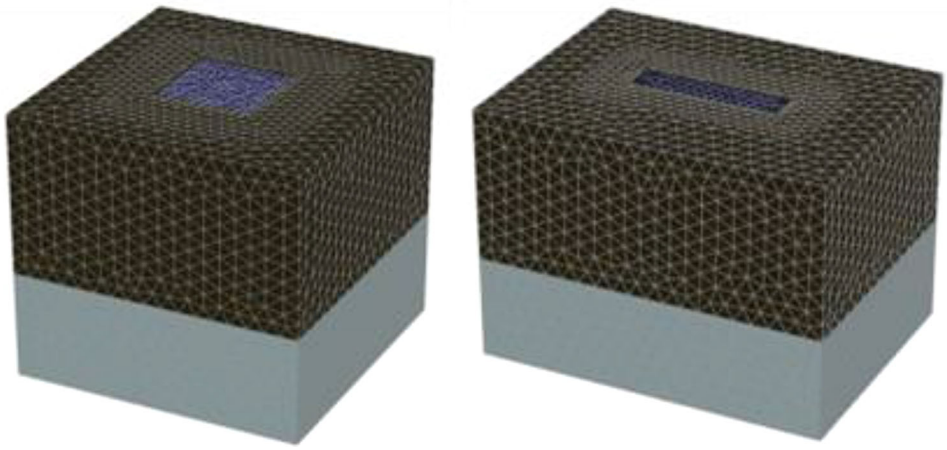

Fig. 15 Mesh element size and mesh density distribution in the FE analysis

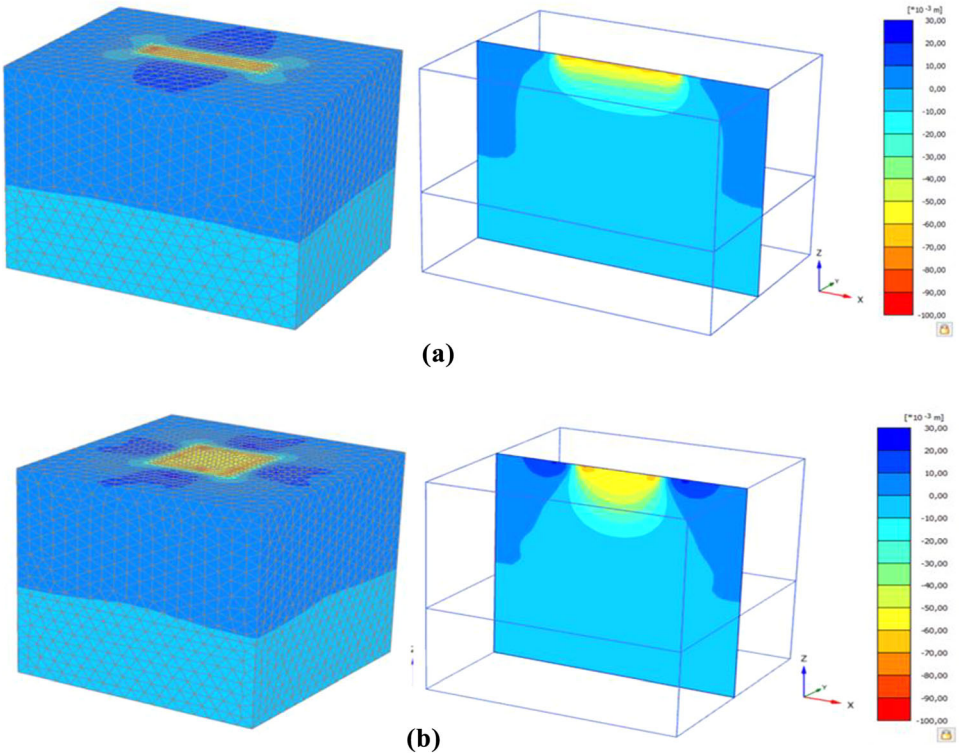

Fig. 16 Vertical displacement contours obtained by FE analysis

swelling at the foundation edges may occur due to local and general shear failure, and the decrease in the vertical load effect toward the bottom of the box decreases the displacements toward the bottom of the box.

Based on Fig. 17 and Table 11, the stress value reached 85.53 kPa on the square footing and 98.12 kPa on the rectangular footing according to the 0.1B method. The stress values corresponding to 100 mm settlement in the test are 187.05 kPa on the square footing and 516.24 kPa on the rectangular footing.

When the test results in Table 12 are examined, the pressure values obtained for 100 mm under the plate are approximately 2.5 times those obtained for 24 mm. The pressure values under the footing are about two times the ones formed under the OS. It has been determined that the pressure values transmitted to the test box boundaries due to the foundation loading are between 2.18 and 3.45 kPa, and it can be said that the measurement values are negligibly low.

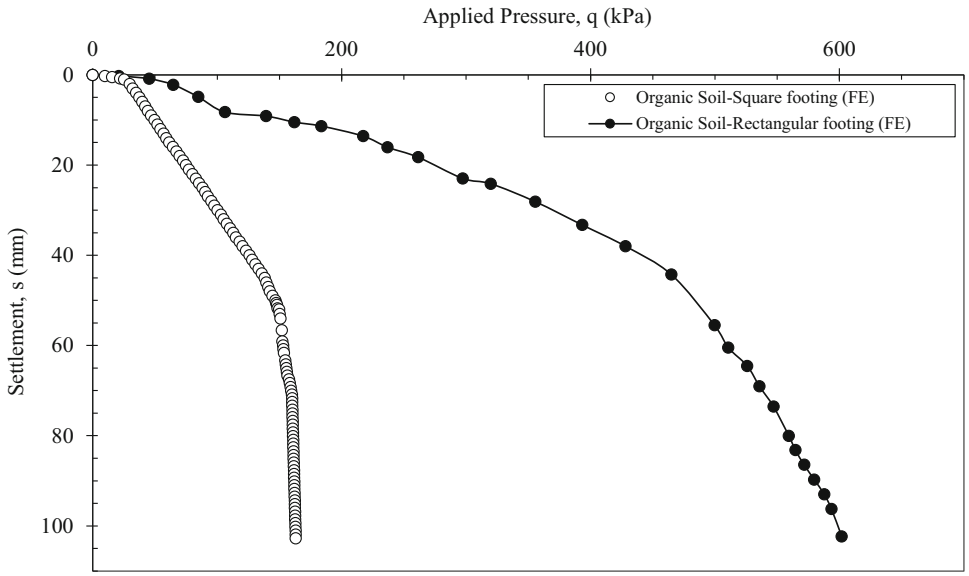

Fig. 17 Applied pressure–settlement curves obtained as a result of FE analysis

Table 11 Calculated bearing capacity values in FE analysis

Footing types	Bearing capacity values (kPa)		
	8 mm (0.1B)	24 mm (0.1B)	100 mm (Ultimate)
Square footing	–	85.53	187.05
Rectangular footing	98.12	–	516.24

Table 12 Soil pressure values obtained as a result of FE analysis

Footing types	Settlement (mm)	Pressure below footing (kPa)	Pressure between the layer of organic soil and sand (kPa)	Pressure at the boundaries of the test box (kPa)	
				Length of the box (kPa)	Width of the box (kPa)
Square footing	24 mm	11.38	6.11	2.18	–
	100 mm	19.83	10.63	3.02	–
Rectangular footing	8 mm	12.24	6.75	2.34	2.65
	100 mm	18.57	12.65	3.16	3.45

6 Conclusions and Discussion

This study can be evaluated as the first attempt to examine the disturbance effect of organic soil on the bearing capacity. The results obtained by model tests, field tests, and numerical studies are evaluated as follows.

The bearing capacity values of DOS are low compared to UOS. In other words, it has been observed that the disturbance of organic soil causes losses of up to 42% in the bearing capacity. The soil's strength reduces the soil's degree of disturbance (change in its natural structure, hence the arrangement/shape of its grains) [46].

Upon inspecting the cross-sectional views of the disturbed and undisturbed organic soil after model tests, movements similar to local shear failure were observed in the UOS. In contrast, soil movements similar to punching failure were observed in the DOS. This situation may be related to the degree of disturbance of the soil and the decrease in soil strength.

The load transmitted to the pressure sensors in the DOS during loading is slightly higher than in the UOS which is attributed to the effect of semi-degraded animal and plant parts.

While the bearing capacity values calculated by different empirical methods are very close to the test results obtained with the disturbed model tests, it has been observed that there are differences up to 1.5 times with the test results obtained with the disturbed model tests. This situation can be related to the fact that the positive effect of the intact fibers in the UOS on the bearing capacity is not considered in analytical methods.

When the DCP and FVT results applied in three different situations were examined, it was observed that the same depth was reached in fewer blows as the degree of disturbance on the soil increased. Once more, this situation results from a soil strength reduction due to organic soil disturbance.

The bearing capacity values obtained by FEA are 16% lower on average than the bearing capacity values obtained

as a result of the undisturbed model tests, an average of 29% higher than the bearing capacity values obtained with the disturbed model tests, and an average 25% higher than the bearing capacity values obtained by analytical methods.

This study is the first attempt to examine organic soils with field, numerical analyses, and undisturbed/disturbed lab-scale model tests. As a result of model tests, field tests, and numerical studies, it has been observed that huge bearing capacity losses (up to 50%) can occur due to the disturbance of OS from soft soils. It has been revealed that to reflect the geotechnical properties of the OS in the field conditions, it is vital to collect the samples in an undisturbed manner without significant damage to the fiber structure in the soil grains. In addition, the bearing capacity values obtained from FE analysis were significant in the preliminary evaluation for OS. However, it should be noted that taking soil samples from the field, transporting them to the laboratory, and keeping them until the test is critical in determining the organic soil's input parameters (index and engineering properties).

In addition to this study, the bearing capacity losses of OS exposed to repetitive or dynamic loads (earthquakes) under the effect of cyclic loads/dynamic loads can be examined in detail with the site, laboratory, and FE analysis.

Acknowledgements This study was funded through the "The Scientific and Technological Research Council of Turkey" (TUBITAK). Project Type; The Scientific and Technological Research Projects Funding Program (1001) and Project No. 119M974.

Funding This article is funded by Türkiye Bilimsel ve Teknolojik Araştırma Kurumu, 119M974, Zulkuf Kaya.

Data availability All data, models, and code generated or used during the study appear in the submitted article. Some or all data, models, or codes that support the findings of this study are available from the corresponding author upon reasonable request.

Declarations

Conflict of interest The authors declare that they have no known competing financial interests or personal relationships that could have appeared to influence the work reported in this paper.

References

1. Long M (2005) Review of peat strength, peat characterisation and constitutive modelling of peat with reference to landslides. Stud Geotech Mech 27(3–4):67–90
2. Dehghanbanadaki A, Sotoudeh MA, Golpazir I, Keshtkarbanaeemoghadam A, Ilbeigi M (2019) Prediction of geotechnical properties of treated fibrous peat by artificial neural networks. Bull Eng Geol Environ 78(3):1345–1358. https://doi.org/10.1007/s10064-017-1213-2
3. Paul A, Hussain M (2019) An experiential investigation on the compressibility behavior of cement-treated Indian peat. Bull Eng Geol Environ 79:1471–1485. https://doi.org/10.1007/s10064-019-01623-x
4. Kaya Z (2016) Effect of slag on stabilization of sewage sludge and organic soil. Geomech Eng 10(5):689–707. https://doi.org/10.12989/gae.2016.10.5.689
5. Chen C, Zhou Z, Kong L, Zhang X, Yin S (2018) Undrained dynamic behaviour of peaty organic soil under long-term cyclic loading, Part I: experimental investigation. Soil Dyn Earthq Eng 107:279–291. https://doi.org/10.1016/j.soildyn.2018.01.012
6. Moayedi H, Nazir R (2018) Malaysian experiences of peat stabilization, state of the art. Geotech Geol Eng 36(1):1–11. https://doi.org/10.1007/s10706-017-0321-x
7. Wong LS, Hashim R, Ali F (2013) Improved strength and reduced permeability of stabilized peat: Focus on application of kaolin as a pozzolanic additive. Constr Build Mater 40:783–792. https://doi.org/10.1016/j.conbuildmat.2012.11.065
8. Hamed M, Emirler B, Canakci H, Yildiz A (2020) 3D numerical modeling of a single pipe pile under axial compression embedded in organic soil. Geotech Geol Eng 38(5):4423–4434. https://doi.org/10.1007/s10706-020-01299-1
9. Huat BBK, Asadi A, Kazemian S (2009) Experimental investigation on geomechanical properties of tropical organic soils and peat. Am J Eng Appl Sci 2(1):184–188. https://doi.org/10.3844/ajeassp.2009.184.188
10. Dahl KR, Boulanger RW, Dejong JT, Driller MW (2010) Effects of sample disturbance and consolidation procedures on cyclic strengths of intermediate soils. In: Fifth International Conferences on Recent Advances in Geotechnical Earthquake Engineering and Soil Dynamics in Honor of I. M. Idriss 1–21. May 24–29, 2010; San Diego, CA
11. Amundsen HA, Thakur V, Emdal A (2016) Sample disturbances in block samples of low plastic soft clays. In: Proceedings of the 17th Nordic Geotechnical Meeting Challenges in Nordic Geotechnics pp 159–68. Iceland
12. Viana da Fonseca A, Pineda J (2017) Getting high-quality samples in 'sensitive' soils for advanced laboratory tests. Innov Infrastruct Solut 2:1–42. https://doi.org/10.1007/s41062-017-0086-3
13. Karlsrud K, Hernandez-Martinez FG (2013) Strength and deformation properties of Norwegian clays from laboratory tests on high-quality block samples. Can Geotech J 50(12):1273–1293. https://doi.org/10.1139/cgj-2013-0298
14. Amundsen HA, Thakur V, Emdal A (2015) Comparison of two sample quality assessment methods applied to oedometer test results. In: 6th International Symposium on Deformation Characteristics of Geomaterials pp 923–30. Argentina
15. Amundsen HA, Emdal A, Sandven R, Thakur V (2015) On engineering characterisation of a low plasticity sensitive clay. In: GEOQuébec 2015-Challenges from North to South Québec, Canada
16. Hajj AR (1990) The simulation of sampling disturbance and its effects on the deformation behaviour of clays. [Doctoral dissertation]. University of Sheffield
17. Chung C-K (2008) Lecture notes-engineering properties of soils. Seoul university department of civil and environmental engineering. https://ocw.snu.ac.kr/node/2139. Accessed 15 Jan 2023
18. ASTM International (2019) D2216-19 Standard test methods for laboratory determination of water (moisture) content of soil and rock by mass. https://doi.org/10.1520/D2216-19
19. ASTM International (2014) D854-14 standard test methods for specific gravity of soil solids by water pycnometer. https://doi.org/10.1520/D0854-14
20. ASTM International (2017) D2487-17e1 standard practice for classification of soils for engineering purposes (Unified Soil Classification System). https://doi.org/10.1520/D2487-17E01

21. Mesri G, Ajlouni M (2007) Engineering properties of fibrous peats. J Geotech Geoenviron 133(7):850–866. https://doi.org/10.1061/(ASCE)1090-0241(2007)133:7(850)
22. Zainorabidin A, Mansor SH (2016) Investigation on the shear strength characteristic at Malaysian peat. ARPN J Eng Appl Sci 11(3):1600–1606
23. Andresen A, Kolstad P (1979) The NGI 54-mm samplers for undisturbed sampling of clays and representative sampling of coarser materials. In: Proceedings of the international symposium of soil sampling, state of the art on current practice of soil sampling, pp 13–21
24. Lunne T, Berre T, Strandvik S (1997) Sample disturbance effects in soft low plastic Norwegian clay. In: Symposium on Recent Developments in Soil and Pavement Mechanics, Rio de Janeiro, pp 81–102
25. Kaya Z, Erol A (2021) Comparison of bearing capacities of undisturbed organic soils by empirical relations and 2D finite element analysis. Arab J Geosci. https://doi.org/10.1007/s12517-021-08364-w
26. ASTM International (2020) D2435 standard test methods for one-dimensional consolidation properties of soils using incremental loading. https://doi.org/10.1520/D2435_D2435M-11R20
27. Lutenegger A, Adams M (1998) Bearing capacity of footings on compacted sand. Fourth Int Conf Case Hist Geotech Eng 36:1216–1224
28. Cerato AB, Lutenegger AJ (2007) Scale effects of shallow foundation bearing capacity on granular material. J Geotech Geoenviron 133(10):1192–1202. https://doi.org/10.1061/(ASCE)1090-0241(2007)133:10(1192)
29. Keskin S, Laman M, Uğur S (2012) Effect of footing dimension on the bearing capacity of shallow foundations on sand. Çukurova Üniversitesi Mühendislik-Mimarlık Fakültesi Dergisi 27(2):37–46
30. Briaud JL, Jeanjean P (1994) Load settlement curve method for spread footings on sand. J Geotech Geoenviron 133(8):905–920
31. Terzaghi K (1943) Theoretical soil mechanics. New York
32. Meyerhof GG (1951) The ultimate bearing capacity of foundations. Geotechnique 2(4):301–332. https://doi.org/10.1680/geot.1951.2.4.301
33. Hansen JB (1970) A revised and extended formula for bearing capacity. Bull Danish Geotech Inst 28(28):5–11
34. Skempton AW (1984) The Bearing Capacity of Clays. Selected Papers on Soil Mechanics:50–9. https://doi.org/10.1680/sposm.02050.0008
35. Rahim A, Prasad SN, George KP (2004) Dynamic cone penetration resistance of soils—theory and evaluation. Geotechnical Engineering for Transportation Projects. 1755-66
36. Kim H (2014) Dynamic analysis of dynamic cone penetration test for subgrade compaction assessment. [Doctoral dissertation]. Purdue University
37. Scala AJ (1956) Simple methods of flexible pavement design using cone penetrometers. NZ Eng 11(2):34–44
38. ASTM International (2023) D6951/D6951M-18 standard test method for use of the dynamic cone penetrometer in shallow pavement applications. https://doi.org/10.1520/D6951_D6951M-18R23
39. Muntohar AS, Rahman ME, Hashim R, Islam MS (2013) A numerical study of ground improvement technique using group of soil-column on peat. Pertanika J Sci Technol 21(1):625–634
40. Anouar S, Zeineddine B (2022) Reinforced soft soil by CSV with/without polypropylene fiber: experimental and numerical analysis. Frat ed Integrita Strutt 59:374–395. https://doi.org/10.3221/IGF-ESIS.59.25
41. Feng R, Wang L, Wei K, Zhao J (2021) Consolidation settlement of soil foundations containing organic matters subjected to embankment load. Geomech Eng 24(1):43–55. https://doi.org/10.12989/gae.2021.24.1.043
42. Gniel J, Bouazza A (2008) Numerical modeling of small-scale geogrid encased sand column tests. In: Proceedings of the Second International Workshop on Geotechnics of Soft Soils, Scotland, pp 143–149
43. Nikitin A (2018) Numerical simulation of sand fill to allow operation of pile driving rigs on peaty soil. IOP Conf Ser Mater Sci Eng 463(4):042045
44. Savidis SA, Rackwitz F, Schüßler M (2008) Design and construction of granular soil columns for ground improvement of very soft soils for road embankments. In: 6th International Conference on Case Histories in Geotechnical Engineering 7–17. August 11–16, 2018; Arlington, VA
45. PLAXIS Company (2021) PLAXIS CONNECT Edition V21. General information manual
46. Nhuan BD (1981) Sample disturbance and its effects on the geotechnical properties of clays. Swedish Geotechnical Institute-SGI Varia 68. http://www.diva-portal.se/smash/get/diva2:1300201/FULLTEXT01.pdf

Springer Nature or its licensor (e.g. a society or other partner) holds exclusive rights to this article under a publishing agreement with the author(s) or other rightsholder(s); author self-archiving of the accepted manuscript version of this article is solely governed by the terms of such publishing agreement and applicable law.